

Non-iterative One-step Solution for Point Set Registration Problem on Pose Estimation without Correspondence

Yijun Yuan¹, Dorit Borrmann², Andreas Nüchter² and Sören Schwertfeger¹

Abstract—In this work, we propose to directly find the one-step solution for the point set registration problem without correspondences. Inspired by the Kernel Correlation method, we consider the fully connected objective function between two point sets, thus avoiding the computation of correspondences. By utilizing least square minimization, the transformed objective function is directly solved with existing well-known closed-form solutions, e.g., singular value decomposition, that is usually used for given correspondences. However, using equal weights of costs for each connection will degenerate the solution due to the large influence of distant pairs. Thus, we additionally set a scale on each term to avoid high costs on non-important pairs. As in feature-based registration methods, the similarity between descriptors of points determines the scaling weight. Given the weights, we get a one step solution. As the runtime is in $O(n^2)$, we also propose a variant with keypoints that strongly reduces the cost. The experiments show that the proposed method gives a one-step solution without an initial guess. Our method exhibits competitive outlier robustness and accuracy, compared to various other methods, and it is more stable in case of large rotations. Additionally, our one-step solution achieves a performance on-par with the state-of-the-art feature based method TEASER.

I. INTRODUCTION

The point set registration problem has been explored for several decades. Various techniques have been invented, focusing on both efficiency and accuracy. As discussed in [1], it is extremely hard to find the optimal transformation \mathbf{T} and correspondence matrix \mathbf{P} simultaneously. The problem has been addressed in [1] by alternating the optimization of \mathbf{T} and \mathbf{P} .

In recent decades, a multitude of algorithms have been proposed on 3D registration. They are divided into rigid and non-rigid algorithms [2] and work either iteratively to solve for the transformation matrix with repeatedly matched points [3], [4], [5], [6], [7] or treat the problem as an optimization program that omits the necessity of computing correspondences [8], [9], [10]. With the high capability of regression methods for Deep Neural Networks, there are some attempts to directly solve the transformation with deep neural networks. Researchers start to seek for approaches that directly predict the transformation [11]. However, those trained models highly rely on the learning data that make it both very costly and not reliable to cases that are not covered by the space of training data.

¹Yijun Yuan and Sören Schwertfeger with the School of Information Science and Technology, ShanghaiTech University, China. [yuanwj|soerensch]@shanghaitech.edu.cn

²Dorit Borrmann, Andreas Nüchter are with the Department of Informatics VII – Robotics and Telematics, Julius-Maximilians-University Würzburg, Germany.

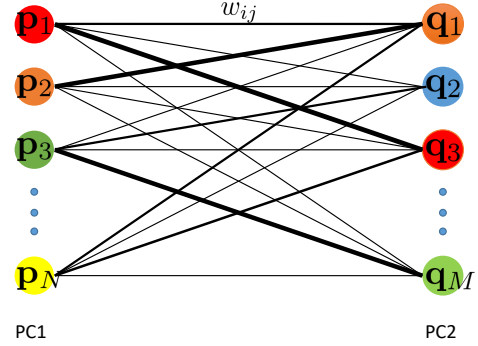


Fig. 1: Full connection between two point sets. Each edge is a weighted Euclidean squared distance term in our object function, given a proper $w_{i,j}$ to scale the cost term of the pair (i, j) . The thickness of the lines reflect the similarity (weight) of pairs.

This paper presents a direct solution to the point cloud registration problem without the need of a trained model. There are two problems to address: Correspondence computation and optimization of the objective function. Kernel correlation (KC) [8] is one of the most common registration methods that solves the problem without known correspondences by minimizing the full connection cost between two point sets. It is generally in the form $-\mathcal{K}(\mathbf{X}, \mathbf{Y})$ with \mathcal{K} being the kernel. Inspired by the distribution distance, we consider the full connection loss as a good way to omit the correspondence computation.

Aiming at a one-step solution, we first review closed-form results. Given correspondences, there are four known possibilities [12], [13], [14], [15]. The singular value decomposition (SVD) is widely used for computing the optimal rotation \mathbf{R} and afterwards the optimal translation \mathbf{t} [15]. Our full connection function builds on this least square solution.

But if each cost term has an equivalent effect on the objective function, the method will fail. In the KC method, the costs between very distant points only has a tiny impact due to its kernel function. However, in the least square case, large distances will dominate the system and thus do not perform well. Therefore, we properly weigh each cost term to suppress the influence of distant point pairs. The weights consider the similarity between two points. Fig. 1 illustrates the full connection, weights are set according to a similarity measure.

In the following, we first formulate the problem and show some related solutions. Then our method is detailed in Section III. After that, in Section IV, we present the

experiments for sensitivity to noise, robustness to outliers, and overall accuracy.

II. RELATED WORK

The Iterative Closest Point (ICP) algorithm is the most famous registration method. It has been widely applied to various representations of 3D shapes [4] and is able to align a set of range images into a 3D model [5]. The generalized-ICP [6] even puts point-to-point ICP and point-to-plane ICP into one probabilistic framework. ICP consists of two steps, correspondence search and solving for the optimal transformation.

To speed up the search process, point clouds often are stored in k -d trees. To make it faster, Marden and Guivant [3] propose to use a grid data structure to provide a constant time approximate nearest neighbor search. To achieve better quality for matching, especially of very large point clouds, feature based methods are used. Fast Point Feature Histograms (FPFH) are used to analyze the local geometry around a 3D point and provide a basis for the fast computation of a descriptor [7].

Given known correspondences, the transformation can be computed. Walker et al. use dual number quaternions and formulate it as an optimization problem [12]. With a matrix of sum of products of corresponding point coordinates, Horn computes the optimal rotation from the eigenvector associated to the largest positive eigenvalue [13]. This eigenvector is a unit quaternion representing the rotation.

However, the least square form using a matrix representation of rotation is more common. The problem is formulated as follows: Assume we have two point clouds \mathbf{P} and \mathbf{Q} with $\mathbf{p}_i \in \mathbf{P}|_{i \in \{1, \dots, N\}}$ and $\mathbf{q}_j \in \mathbf{Q}|_{j \in \{1, \dots, M\}}$. Since we have 3D point clouds, $\mathbf{p}_i, \mathbf{q}_j \in \mathbb{R}^3$. Then the optimization task is

$$\min_{\mathbf{R}, \mathbf{t}} \sum_{(i,j) \in \mathcal{C}} \|\mathbf{R}\mathbf{p}_i + \mathbf{t} - \mathbf{q}_j\|^2 \quad (1)$$

where \mathbf{R} , \mathbf{t} are the rotation matrix and translation vector to transform \mathbf{P} into the coordinate system of \mathbf{Q} . \mathcal{C} is the set of correspondences.

With a more widely used orthogonal matrix representation for the rotation, Horn et al. [14] formulate a least square problem and propose a solution using a 3-by-3 matrix. Also relying on a matrix representation, Arun et al. [15] resort to the SVD to solve for the rotation as a multiplication of the two resulting orthonormal matrices.

However, in ICP and related methods, the correspondences have to be recomputed each iteration. To avoid this, the KC method [8] uses an objective function that fully connects the point clouds:

$$\min_{\mathbf{R}, \mathbf{t}} \sum_{i=1}^N \sum_{j=1}^M e^{-\frac{\|\mathbf{R}\mathbf{p}_i + \mathbf{t} - \mathbf{q}_j\|^2}{2\sigma^2}} \quad (2)$$

if Gaussian distances are chosen. In each term of the summation, a robust function, the Gaussian distance, has been utilized. Similar to Maximum Mean Discrepancy (MMD), KC evaluates the distance between two distributions. Thus

it shows better sensitivity to noise and is more robust than ICP-like methods. Some recent publications do not rely on correspondences. Myronenko and Song [9] represent point clouds with Gaussian mixture models and solve the transformation by aligning the model centroids. Zheng et al. [10] build a continuous distance field for a fixed model and align the other point set model to minimize the energy iteratively. Yang et al. [16] reformulate the registration as a truncated least squares estimation (TEASER) which is thus robust with extremely wrong correspondences.

III. METHODOLOGY

Actually, both Equations (1) and (2) have their benefits. While needing to compute the correspondences, Eq. (1) has a closed-form solution. The KC loss Eq. (2) omits the necessity of finding the correspondences.

We intend to use both full connection and the least square form. However, just replacing the kernel with the quadratic distance will not work due to the distant pairs that will dominate the loss. As discussed in [8], the gradient of the quadratic function is very sensitive to outliers, so a more robust function, the Gaussian kernel, has been utilized. To avoid the fast increase of the gradient, we use additional weights to rebalance each quadratic term in the full connection. The formula is a summation of square distances for each fully connected point pair. The weight $w_{i,j}$ in the range $(0, 1]$ has been assigned for each term.

$$\min_{\mathbf{R}, \mathbf{t}} \sum_{i=1}^N \sum_{j=1}^M w_{i,j} \|\mathbf{R}\mathbf{p}_i + \mathbf{t} - \mathbf{q}_j\|^2 \quad (3)$$

Please note that one problem of Gaussian kernel distances in the KC method is, that σ has to be properly set according to the scale of the data. We use the square distance, as it is invariant to scale [17]. However, to have the desired suppression effect, weights cannot be arbitrarily chosen. We will discuss the weights in Section III-B.

A. Solving the Transformation

For the weighted function (3), there is a full connection with quadratic distance between every point $\mathbf{p} \in \mathbf{P}$ and $\mathbf{q} \in \mathbf{Q}$. Then the problem is to reformulate Eq. (3) with full connection as correspondences. The new point sets $(\mathcal{X}, \mathcal{Y})$ are of size NM and each pair is a connection.

The optimal solution is obtained with any algorithm that computes the transformation. To make the paper self-contained, we choose the SVD [15], also detailed in [18]. Let $\mathcal{X} = \{\mathbf{p}'_1, \dots, \mathbf{p}'_{NM}\}$, $\mathcal{Y} = \{\mathbf{q}'_1, \dots, \mathbf{q}'_{NM}\}$, the problem is formulated as

$$(\mathbf{R}, \mathbf{t}) = \underset{\mathbf{R} \in SO(d), \mathbf{t} \in \mathbb{R}^d}{\operatorname{argmin}} \sum_{i=1}^{NM} w_i \|(\mathbf{R}\mathbf{p}'_i + \mathbf{t}) - \mathbf{q}'_i\|^2 \quad (4)$$

with known weights $w_i > 0$.

We cancel \mathbf{t} by computing the weighted mean

$$\bar{\mathbf{p}}' = \frac{\sum_{i=1}^{NM} w_i \mathbf{p}'_i}{\sum_{i=1}^{NM} w_i}, \quad \bar{\mathbf{q}}' = \frac{\sum_{i=1}^{NM} w_i \mathbf{q}'_i}{\sum_{i=1}^{NM} w_i} \quad (5)$$

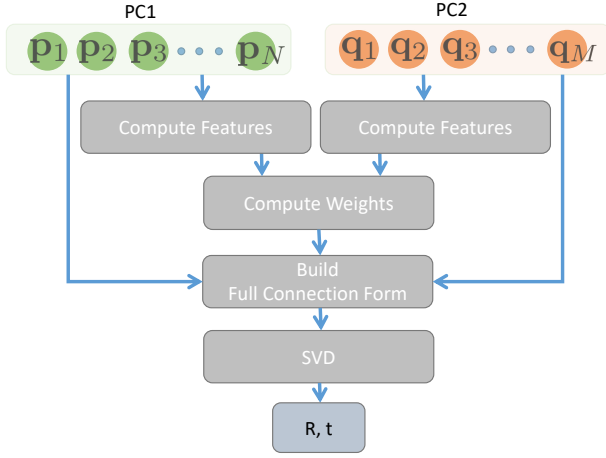


Fig. 2: Pipeline of the proposed method.

and centering the point clouds

$$\mathbf{x}_i := \mathbf{p}'_i - \bar{\mathbf{p}}', \mathbf{y}_i := \mathbf{q}'_i - \bar{\mathbf{q}}'. \quad (6)$$

We can then compute \mathbf{R}

$$\mathbf{R} = \underset{\mathbf{R} \in SO(d)}{\operatorname{argmin}} \sum_{i=1}^{NM} w_i \|\mathbf{R}\mathbf{x}_i - \mathbf{y}_i\|^2. \quad (7)$$

Let \mathbf{X} denote the matrix where \mathbf{x}_i is the i -th column. Similarly, we have \mathbf{Y} . Thus, $\mathbf{X}, \mathbf{Y} \in \mathbb{R}^{3 \times NM}$. \mathbf{W} is a diagonal matrix with $\mathbf{W}_{i,i} = w_i$. The SVD solves it where

$$\mathbf{U}\Sigma\mathbf{V}^T = \mathbf{X}\mathbf{W}\mathbf{Y}^T \quad (8)$$

and the optimal rotation is computed by

$$\mathbf{R} = \mathbf{V}\mathbf{U}^T. \quad (9)$$

When the solution consists of a reflection, i.e., $|\mathbf{V}||\mathbf{U}| < 0$, the last column of \mathbf{V} will be multiplied with -1 before computing the rotation.

Finally, the translation is given as

$$\mathbf{t} = \bar{\mathbf{q}}' - \mathbf{R}\bar{\mathbf{p}}'. \quad (10)$$

B. Weights as Similarity of Feature

To determine the weights, we use $f_{\mathcal{X}}(\mathbf{x})$ to denote a function that extracts a feature descriptor of the point \mathbf{x} from the point cloud \mathcal{X} . Then the similarity is obtained as

$$w_i = e^{-\frac{1}{\beta} \|f_{\mathcal{X}}(\mathbf{p}'_i) - f_{\mathcal{Y}}(\mathbf{q}'_i)\|^2}. \quad (11)$$

The lower the similarity, the lower the weight of the pairs. Thus, the effect of the term on the objective function will be less. In this way, a pair of points with low similarity contributes only a little, as they have a large feature descriptor distance. The constant β in Eq. (11) scales the feature distance. It depends on the selected feature descriptor. We utilize the FPFH [7] for f in our implementation.

In addition to β and f , the feature extraction usually depends on the chosen radius. This implies performance changes when using differently scaled data. To make the

whole algorithm invariant to scale, FPFH is using the k nearest neighbor search for normal and feature extraction. The complete registration pipeline is given in Fig. 2.

C. Time Complexity

The runtime for the proposed method is dominated by two parts: Computing the weights and solving the SVD. For convenience we assume $M = N$. To compute the weight, point descriptors of each point cloud are computed, which takes $\mathcal{O}(Nk \log N)$, where k is the number of neighbors for each point. Then setting up the N^2 weights takes $\mathcal{O}(N^2)$. In the SVD, we first compute the centroid and transform the point cloud to center, which takes $\mathcal{O}(N^2)$, because we have to consider NM terms. Since $\mathbf{W} \in \mathbb{R}^{NM \times NM}$ is a diagonal matrix, the multiplication for $\mathbf{X}\mathbf{W}\mathbf{Y}^T$ is equivalent to scaling each row i of \mathbf{Y}^T with $\mathbf{W}_{i,i}$. Thus, to obtain $\mathbf{X}\mathbf{W}\mathbf{Y}^T$ takes $\mathcal{O}(N^2)$. As $\mathbf{X}\mathbf{W}\mathbf{Y}^T$ is a 3-by-3 matrix, solving the SVD costs only constant time.

Overall, the time complexity of proposed method is with $\mathcal{O}(N^2)$.

D. A Variant: Applying on Point Set of Keypoints

For large point sets, the time complexity of $\mathcal{O}(N^2)$ becomes infeasible. One possible solution is to extract interest points and to apply the full connection cost to the two sets of keypoints.

Using FPFH, the implementation is inexpensive. For each point set with N points, computing the normals takes $\mathcal{O}(Nk \log N)$ and keypoint detection takes $\mathcal{O}(N)$. Assume n points are extracted ($n \ll N$), then weight and SVD computation is done on n points. Overall, we yield $\max(\mathcal{O}(Nk \log N), \mathcal{O}(n^2))$.

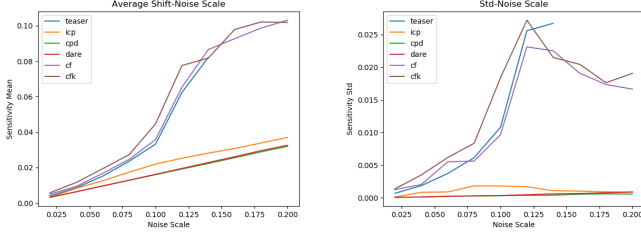
IV. EXPERIMENTS AND RESULTS

We compare the proposed algorithm with ICP, a feature based state-of-the-art algorithm (TEASER), Coherent Point Drift (CPD) and Density Adaptive Point Set Registration (DARE). We call our method Full Connection Form Solution (CF) and CF-keypoint (CFK) (a variant with keypoints) for short.

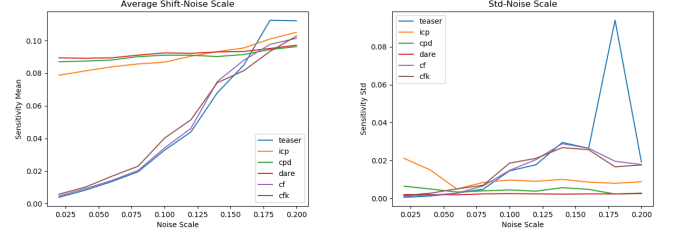
In our experiments, the small 3D object datasets “bunny”, “dragon”, and “Armadillo” (bun000, dragonStandRight.0 and ArmadilloStand_180) from the Stanford website¹ have been used. They are in bounding boxes with side lengths (0.156, 0.153, 0.118), (0.205, 0.146, 0.072) and (0.215, 0.275, 0.258) respectively. They are shown in Fig. 4. With those we evaluate our algorithms w.r.t. its sensitivity to noise, the robustness to outliers, and the accuracy of the registration. The implementation and test code are given in source files that are available in github².

¹<http://graphics.stanford.edu/data/3Dscanrep/>

²Added after acceptance



(a) Small angle, centered



(b) Large angle, not centered

Fig. 3: Sensitivity test. The left two plots show results with small rotation, centered. The right two plots show results with large rotation, not centered. The first and third diagrams show the mean shift to noise scale. The second and forth diagrams show the standard deviation.

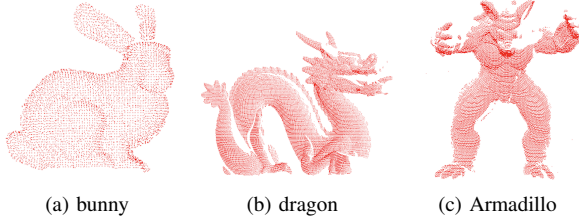


Fig. 4: Three point cloud used for experiments.

A. Settings

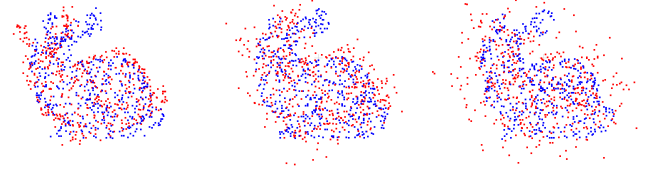
We first sample the point clouds from the meshes using Meshlab [19]. For CPD the open source C++ implementation from the original project [9] is used. We have set its scale and reflection parameters to false. For DARE we use the python implementation of [20]. Its color label and feature label are disabled. We also use TEASER from the TEASER++ implementation [21]. We have implemented CF and CFK using the Point Cloud Library (PCL) [22], where we use its FPFH descriptor and the SIFT keypoint detector. The ICP experiments were also done with PCL. The normal and feature computation in CF and CFK are performed with the same settings, i.e., searching k neighbors. In our implementation we fixed k to 150. In addition, the β used in Eq. (11) is fixed to 100.

We set the ICP parameters with max correspondence distance 0.5, max iteration 1000, transformation epsilon $1e-9$ and Euclidean fitness epsilon 0.05.

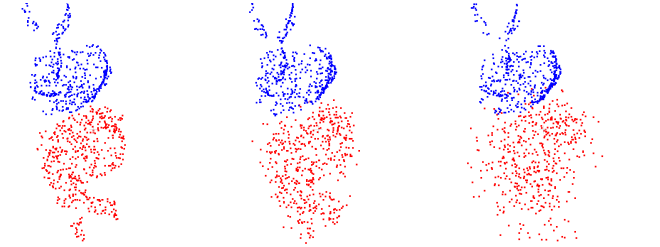
For TEASER, we use the same settings as for the feature descriptor FPFH. In the matcher of TEASER++, the options absolute_scale and crosscheck are selected. The solver is using GNC-TLS with a 1.4 gnc factor, 0.005 rotation cost threshold and 1000 max iterations.

In our experiments, the registration is done using two point clouds PC_a and PC_b , that were generated with added noise or outliers from the original point cloud, as is described in more detail later. We then translate and rotate PC_b to get PC'_b . So the PC_a is our PC1 and PC'_b is our PC2 and our task is to align PC1 to PC2 by solving for the transformation.

In the following experiments PC_b is transformed in two distinct ways to generate PC'_b . Firstly, we apply just a small, random rotation around the point clouds centroid. For the second type of data we apply a large random rotation around



(a) Small angle, centered



(b) Large angle, not centered

Fig. 5: Noise data. Above: centered small angle, below: large angle. From left to right column is with noise standard derivation 0.002, 0.01 and 0.02.

the origin of the dataset, which is not the centroid.

The rotation vector is a concise axis-angle representation, for which both the rotation axis and angle are represented in the same 3-vector. The rotation angle is the length of this vector.

The small rotation vectors have values drawn uniformly from $[-\pi/8, \pi/8)$, while the large rotation vectors are uniformly drawn from $[-\pi/2, \pi/2)$.

B. Sensitivity to Noise

In this experiment we evaluate the effects of different levels of noise on the registration. Each level is tested with

TABLE I: Robustness test: smaller is better.

	Small rotation, centered	Large rotation, not centered
ICP	0.0019 ± 0.0062	0.070 ± 0.023
CPD	$2.4e-09 \pm 1.7e-10$	0.040 ± 0.047
DARE	0.012 ± 0.019	0.053 ± 0.035
TEASER	0.0055 ± 0.0027	0.0057 ± 0.0035
CF	0.0075 ± 0.0028	0.0078 ± 0.0032
CFK	0.0096 ± 0.0043	0.0099 ± 0.0052

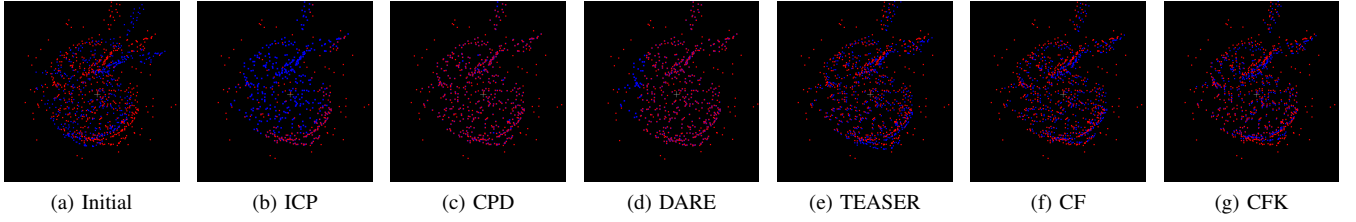


Fig. 6: Robustness test: Example from the small rotation set, centered.

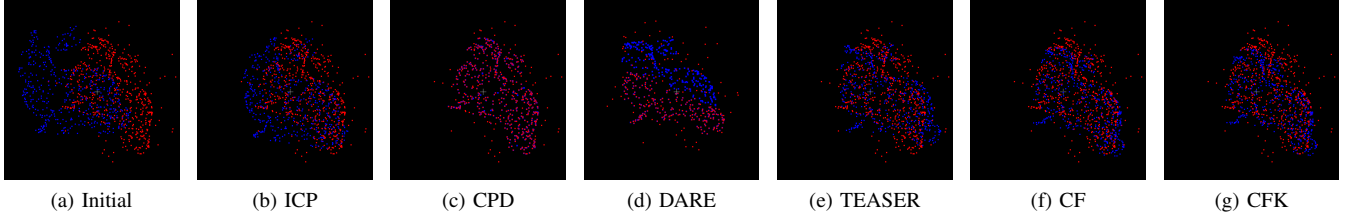


Fig. 7: Robustness test: Medium rotation example from the large rotation set, not centered.

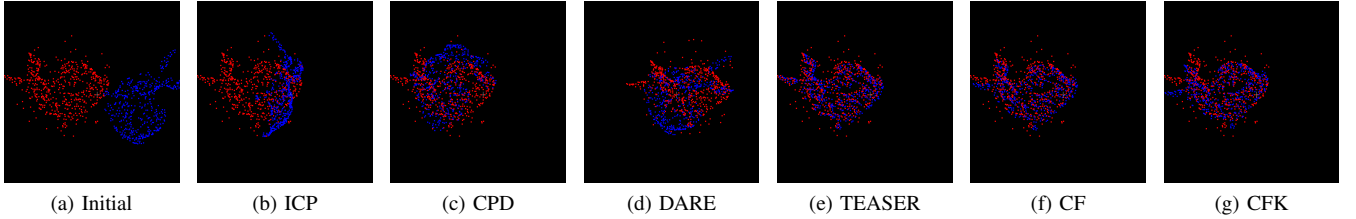


Fig. 8: Robustness test: Large rotation example from the large rotation set, not centered.

30 generated point clouds. Just for this experiment, we fix the large and small rotation angle to two certain values, to be able to concentrate on the effects of the levels of noise and draw the diagrams of Fig. 3. PC1 and PC2 are subsampled to 500 points. For the rotated set PC2, we add zero mean Gaussian noise to each point.

Following the definition of sensitivity [8], we log the mean average shift to evaluate the performance and the standard deviation is utilized as the metric. The noise scale is within the range $(0, 0.02]$. Because the size of the bunny does not exceed 0.3, too large noise will result in dysfunctional feature descriptors. We present the noise data with different noise scale in Fig. 5. The results are given in Fig. 3. In the small angle case of Fig. 3, the TEASER curve breaks due to a low number of correspondences and followed by failure.

For the centered small rotation, ICP, CPD and DARE achieve better average shifts and less sensitivity to noise. For the feature based methods, our CF and CFK perform very similar to TEASER.

However, for the large rotation data, ICP, CPD and DARE fail to align the point clouds, while the feature based methods CF, CFK, and TEASER are able to align with good performance.

C. Robustness to Outliers

Similarly, we also use 500 randomly selected points from the bunny object and perform small and large rotations. Additionally, 100 random points have been uniformly drawn in a spherical way and added to the rotated point set PC2

(with radius 0.2, around the center of sampled point clouds).

Because the first 500 points in each set are also from the same sampled index, we actually know the correspondence in the non-outlier parts. To quantify the robustness, we compute the average shift as in subsection IV-B.

For both large and small rotations, we test 100 times to record the mean and standard deviation. The quantitative evaluation is given in Table I. Selected visualizations of the alignment are presented in Fig. 6, Fig. 7, and Fig. 8. All experiments have been made using randomly drawn rotation vectors.

CPD achieves extremely precise solutions for small rotations, while feature based methods (TEASER, CF, CFK) are similar and are better than ICP and DARE. DARE gives the largest error and standard deviation. For the large rotation case, the feature based methods (TEASER, CF, CFK) perform best and the errors of the remaining methods are several times worse and unstable, since they yield large standard deviations. The performance of our one-step methods are close to TEASER, even though its truncated least square is theoretically more insensitive to spurious data.

We select tests with one centered small rotation and two large rotations for demonstration. In Fig. 6 and Fig. 7, CPD and DARE achieve better alignment, while they fail in Fig. 8. However, our CF and CFK keep similar results, but are affected by the outliers.

TABLE II: Accuracy test: smaller is better.

	Small rotation, centered			Large rotation, not centered		
	bunny	dragon	Armadillo	bunny	dragon	Armadillo
ICP	0.045 ± 0.018	0.045 ± 0.19	0.036 ± 0.022	0.96 ± 1.14	1.09 ± 1.13	1.17 ± 1.15
CPD	0.016 ± 0.0089	0.014 ± 0.0083	0.012 ± 0.0074	1.15 ± 1.30	1.11 ± 1.19	1.13 ± 1.15
DARE	0.020 ± 0.0093	0.016 ± 0.0090	0.016 ± 0.0083	1.30 ± 1.26	1.34 ± 1.22	1.48 ± 1.16
TEASER	0.14 ± 0.076	0.15 ± 0.084	0.16 ± 0.095	0.15 ± 0.096	0.13 ± 0.082	0.14 ± 0.093
CF	0.16 ± 0.10	0.19 ± 0.13	0.28 ± 0.42	0.18 ± 0.14	0.14 ± 0.11	0.15 ± 0.12
CFK	0.26 ± 0.26	0.25 ± 0.22	0.33 ± 0.35	0.26 ± 0.23	0.19 ± 0.18	0.20 ± 0.17

D. Accuracy

Using the same given transformation applied to the original point sets as in subsection IV-C, we achieve rotated models. Then we randomly sample 500 points from both the reference model and the rotated models for testing. In the accuracy test, the three point sets in Fig. 4 (bunny, dragon and Armadillo) are utilized. To evaluate the accuracy, deviations from the identity matrix [23] are computed:

$$ACC_{\mathbf{R}_{gt}}(\mathbf{R}_{\text{predicted}}) = \|\mathbf{I} - \mathbf{R}_{\text{predicted}}\mathbf{R}_{gt}^T\|_F$$

It is a distance measure using the Frobenius norm of a matrix, where \mathbf{R}_{gt} is the given rotation and $\mathbf{R}_{\text{predicted}}$ is the predicted rotation.

Accuracy results are given in Table II. For the centered small rotation case, we observe that CPD also achieves the best score while TEASER, CF and CFK are on the same level. For large rotations, CPD becomes unstable, which results in much larger average rotation distances and their standard deviations. The feature based methods still show close results in different cases. Our one-step solution achieves similar result to the truncated least square method TEASER.

V. DISCUSSION

From the experiments, we find that the feature based algorithms (TEASER, CF, CFK) are more sensitive to noise than the other approaches. Though with very small initial rotation, the noise still has impact on the result. In the outliers test, CPD yields very precise results. The one-step CF algorithm scores close to state-of-the-art TEASER.

However, we also test with large rotation angles and observe, that the feature based algorithms are not affected, which is shown by their very close results in the curves and tables, while the remaining methods fail or have large errors.

We also try our method on the Lecture Hall dataset³. It is a small lecture hall with approx 60 seats and it was scanned from two vantage points close to corners by a high-end Riegl VZ-400 laser scanner with an angular resolution horizontal and vertical of 0.04 deg. One of the scans has two people in it, holding a blanket, while the other does not, thus the scene wasn't static. After sub-sampling, we select 30,000 points randomly from each of the two scans, which are shown in Fig. 9a. We apply CFK on the data and it fails to align the point cloud as seen in Fig. 9b. In our previous experiment, the algorithm is capable to align point clouds from the same distribution. While in such lecture hall case, the missing data

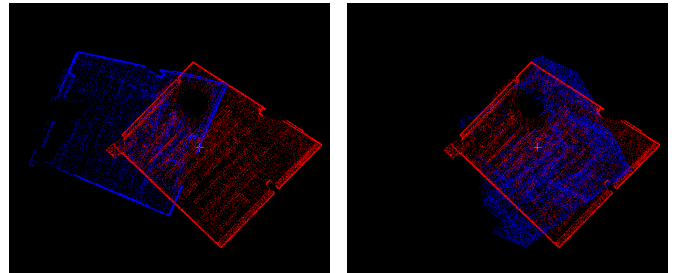
on its corresponding region of the other induce additional error to the one-step solved solution. However, trimmed correspondence and truncated loss are able to solve such case iteratively. Thus, our following work will focus on the distinctiveness of descriptors and more complicated weight designation on this one-step solution. This way the method will be applicable to various kinds of data.

VI. CONCLUSIONS

In this paper we have proposed a new solution to the point set registration problem that does not require correspondences. From our survey, this is the first algorithm that directly provides accurate registrations in a non-iterative one-step setup, where the derived formulas have closed-form solution. Future work will focus on investigating different feature descriptors and weights to achieve better robustness for non-identical distribution data. The experiments in this paper demonstrate competing performance to various methods in robustness to outliers and accuracy. The feature based algorithms (TEASER, CF, CFK) are more sensitive to noise compared to the non-feature based methods due to defunctioning descriptors. Overall, our one-step solution, CF and CFK provide close performance to state-of-the-art TEASER with respect to noise, outliers and accuracy. The non-feature based methods fail or give much worse results while our methods are more stable at large rotations and thus achieve better scores and standard deviations.

ACKNOWLEDGEMENTS

The authors would like to thank Heng Yang and Luca Carlone from Massachusetts Institute of Technology for providing the TEASER code and discussing the topic. This work was supported by a German Academic Exchange Service (DAAD) scholarship granted to Yijun Yuan.



(a) Initial state.

(b) Align two frames.

Fig. 9: Align the Lecture hall data with partial overlap.

³<http://kos.informatik.uni-osnabrueck.de/3Dscans/>

REFERENCES

- [1] H. Li and R. Hartley, "The 3d-3d registration problem revisited," in *2007 IEEE 11th international conference on computer vision*. IEEE, 2007, pp. 1–8.
- [2] B. Bellekens, V. Spruyt, R. Berkvens, and M. Weyn, "A survey of rigid 3d pointcloud registration algorithms," in *AMBIENT 2014: the Fourth International Conference on Ambient Computing, Applications, Services and Technologies, August 24-28, 2014, Rome, Italy, 2014*, pp. 8–13.
- [3] S. Marden and J. Guivant, "Improving the performance of icp for real-time applications using an approximate nearest neighbour search," in *Proceedings of the Australasian Conference on Robotics and Automation, Wellington, New Zealand, 2012*, pp. 3–5.
- [4] P. J. Besl and N. D. McKay, "Method for registration of 3-d shapes," in *Sensor Fusion IV: Control Paradigms and Data Structures*, vol. 1611. International Society for Optics and Photonics, 1992, pp. 586–607.
- [5] S. Fantoni, U. Castellani, and A. Fusiello, "Accurate and automatic alignment of range surfaces," in *2012 Second International Conference on 3D Imaging, Modeling, Processing, Visualization & Transmission*. IEEE, 2012, pp. 73–80.
- [6] A. Segal, D. Haehnel, and S. Thrun, "Generalized-icp," in *Robotics: science and systems*, vol. 2, no. 4, 2009, p. 435.
- [7] R. B. Rusu, N. Blodow, and M. Beetz, "Fast point feature histograms (fpfh) for 3d registration," in *2009 IEEE International Conference on Robotics and Automation*. IEEE, 2009, pp. 3212–3217.
- [8] Y. Tsin and T. Kanade, "A correlation-based approach to robust point set registration," in *European conference on computer vision*. Springer, 2004, pp. 558–569.
- [9] A. Myronenko and X. Song, "Point set registration: Coherent point drift," *IEEE transactions on pattern analysis and machine intelligence*, vol. 32, no. 12, pp. 2262–2275, 2010.
- [10] B. Zheng, R. Ishikawa, T. Oishi, J. Takamatsu, and K. Ikeuchi, "A fast registration method using ip and its application to ultrasound image registration," *IPSN Transactions on Computer Vision and Applications*, vol. 1, pp. 209–219, 2009.
- [11] S. Miao, Z. J. Wang, and R. Liao, "A cnn regression approach for real-time 2d/3d registration," *IEEE transactions on medical imaging*, vol. 35, no. 5, pp. 1352–1363, 2016.
- [12] M. W. Walker, L. Shao, and R. A. Volz, "Estimating 3-d location parameters using dual number quaternions," *CVGIP: Image Understanding*, vol. 54, pp. 358 – 367, November 1991.
- [13] B. K. P. Horn, "Closed-form solution of absolute orientation using unit quaternions," *Journal of the Optical Society of America A*, vol. 4, no. 4, pp. 629 – 642, April 1987.
- [14] B. K. P. Horn, H. M. Hilden, and S. Negahdaripour, "Closed-form solution of absolute orientation using orthonormal matrices," *Journal of the Optical Society of America A*, vol. 5, no. 7, pp. 1127 – 1135, July 1988.
- [15] K. S. Arun, T. S. Huang, and S. D. Blostein, "Least square fitting of two 3-d point sets," *IEEE Transactions on Pattern Analysis and Machine Intelligence*, vol. 9, no. 5, pp. 698 – 700, September 1987.
- [16] H. Yang and L. Carlone, "A polynomial-time solution for robust registration with extreme outlier rates," *arXiv preprint arXiv:1903.08588*, 2019.
- [17] F. Fleuret and H. Sahbi, "Scale-invariance of support vector machines based on the triangular kernel," in *3rd International Workshop on Statistical and Computational Theories of Vision*, 2003, pp. 1–13.
- [18] O. Sorkine, "Least-squares rigid motion using svd," *Technical notes*, vol. 120, no. 3, p. 52, 2009.
- [19] P. Cignoni, M. Callieri, M. Corsini, M. Dellepiane, F. Ganovelli, and G. Ranzuglia, "Meshlab: an open-source mesh processing tool," in *Eurographics Italian chapter conference*, vol. 2008, 2008, pp. 129–136.
- [20] F. Järemo Lawin, M. Danelljan, F. Shahbaz Khan, P.-E. Forssén, and M. Felsberg, "Density adaptive point set registration," in *Proceedings of the IEEE Conference on Computer Vision and Pattern Recognition*, 2018, pp. 3829–3837.
- [21] H. Yang, J. Shi, and L. Carlone, "Teaser: Fast and certifiable point cloud registration," *arXiv preprint arXiv:2001.07715*, 2020.
- [22] R. B. Rusu and S. Cousins, "Point cloud library (pcl)," in *2011 IEEE international conference on robotics and automation*, 2011, pp. 1–4.
- [23] P. M. Larochelle, A. P. Murray, and J. Angeles, "A distance metric for finite sets of rigid-body displacements via the polar decomposition," *Journal of Mechanical Design*, vol. 129, no. 8, pp. 883–886, 2007.